AD-A187 350 COUPLED FE AND HIE METHOD FOR EXTERIOR ACOUSTICS OF AXISYMMETRIC SHELLS(U) ADMIRALTY RESEARCH ESTABLISHMENT TEDDINGTON (ENGLAND) J W JAMES JUL 87 1/1

UNCLASSIFIED ARE-TM-(UHA)-87506 F/G 20/1 NL

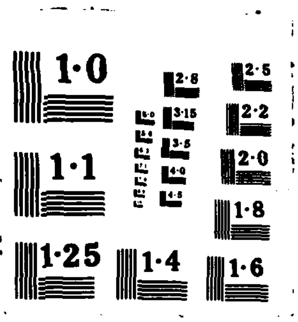
1·0
2·8
2·5
3·2
2·2
3·6
2·0
4·0
1·1
1·8
1·25
1·4
1·6

2

AD-A187 350

ARE TM(UHA)87506

# COUPLED FE AND HIE METHOD FOR EXTERIOR ACOUSTICS OF AXISYMMETRIC SHELLS

BY

J H JAMES

Summary

A conical shell finite element is used to model the shell and the exterior Helmholtz integral equation the fluid, the displacements and pressure being represented by Fourier series expansions in the circumferential coordinate. The dynamic stiffness matrix of the system is obtained by combining the separate dynamic stiffness matrices of the fluid and structure, using 'normal' coordinates alone to save computer time. The excitation is either a time-harmonic point force or a plane wave incident at an oblique angle. In order to validate the problem formulation and computer programs, numerical results of far-field sound radiation from a spherical elastic shell are compared with those from a closed-form shell theory. ([illegible] Great Br[illegible] mechanical [illegible] acoustic excitation).

24 pages
3 figures

ARE (Teddington)
Queen's Road
TEDDINGTON Middlesex TW11 OLN

July 1987

## LIST OF CONTENTS

## 1. INTRODUCTION

A previous Technical Memorandum [1] describes the method of dynamic stiffness coupling, using normal coordinates alone to couple the matrix equations of motion of the structure and fluid, as a potentially useful tool for solving radiation and scattering problems of submerged axisymmetric shell structures which are subjected to axisymmetric excitation. The conical shell element was used model the shell and the interior Helmholtz integral equation the exterior fluid. It recommended that the work should be extended to include the case of general excitation in which the field quantities of interest are expanded as Fourier series in the the circumferential coordinate.

It is the aim of the work contained herein to present the mathematical formulation of the problem of the acoustics of axisymmetric shell structures, which are subjected to asymmetric excitations, and to demonstrate numerically, by comparisons with an exact theory, that a particular Fortran program implementation is a useful tool for research studies.

For completeness, this Technical Memorandum includes much of the work contained in the previous study [1], which publication is now out of date. The derivation of the matrix equations of motion is given without elaboration and with minimal explanation, and a good working knowledge of the finite element method and the Helmholtz integral equation is required for a proper understanding of the Memorandum's contents.

## 2. FINITE ELEMENT METHOD

A finite element Fortran program [2] is available for the dynamic analysis of axisymmetric thin shell structures whose displacements are represented by Fourier series in the circumferential coordinate, viz.

$$\begin{aligned}
u(r,z,\phi) &= \Sigma_{n=0}^{\infty}\, u_n(r,z)\cos(n\phi) \\
v(r,z,\phi) &= \Sigma_{n=0}^{\infty}\, v_n(r,z)\sin(n\phi) \\
w(r,z,\phi) &= \Sigma_{n=0}^{\infty}\, w_n(r,z)\cos(n\phi) \\
\xi(r,z,\phi) &= \Sigma_{n=0}^{\infty}\, \xi_n(r,z)\cos(n\phi)
\end{aligned} \tag{2.1}$$

in which u, v, w are axial, tangential and radial displacements, and $\xi$ is the meridianal rotation. Time variation $\exp(-i\omega t)$ is to be omitted throughout.

The conical shell element is the basic structural component, its geometry being shown in Figure 1c. The mass and stiffness matrix in the n'th circumferential harmonic have been given by Percy et al [3]. Assembly of the elements gives the system matrix equation

$$[S_n - \omega^2 M_n]\ [X_n] = [F_n] \qquad (2.2)$$
$$4m{*}4m \quad 4m{*}1 \quad 4m{*}1$$

for each harmonic, where m is the number of nodes on the structure; $[S_n]$ and $[M_n]$ are the system stiffness and mass matrices. Numerical inversion of this equation is rapid if the bandwidth is kept small. Thus, given the nodal force excitation vector $[F_n]$, the response vector $[X_n]$ can usually be found without excessive computer run-times.

The Fortran program has been modified to give the 'normal' receptance matrix, which is defined as the normal displacement at surface point 'i' due to unit 'normal' force at surface point 'j'. If [W] and [F] are now defined as matrices of 'normal' displacements and 'normal' forces, in the n'th circumferential harmonic, at the m, say, surface nodes, then

$$[W] = [S_e(\omega)]^{-1}[F] \qquad (2.3)$$
$$m{*}1 \quad m{*}m \quad m{*}1$$

where $[S_e(\omega)]^{-1}$ is the frequency dependent receptance matrix. The inverse of this equation is the dynamic stiffness relation

$$[S_e(\omega)]\ [W] = [F] \qquad (2.4)$$
$$m{*}m \quad m{*}1 \quad m{*}1$$

which is the starting point of the fluid-structure interation matrix analysis.

## 3. HELMHOLTZ INTEGRAL EQUATION

### (a) General

The Helmholtz integral equation for a smooth surface $S_0$ undergoing time-harmonic oscillations in an acoustic fluid is

$$q(\underline{R})p(\underline{R}) = (1/4\pi) \int \{p(\underline{R}_0)\partial G(\underline{R},\underline{R}_0)/\partial N_0 - \rho\omega^2 W(\underline{R}_0)G(\underline{R},\underline{R}_0)\}dS_0 \qquad (3.1)$$

where p is acoustic pressure and W is normal surface displacement. $q(\underline{R})$ is 1.0, 0.5 or 0 depending on whether $\underline{R}$ is exterior to, on, or inside the closed surface $S_0$. $\partial/\partial N_0$ is differentiation in the direction of the outward normal.

$$G(\underline{R},\underline{R}_0) = \exp(ik|\underline{R}-\underline{R}_0|)/|\underline{R}-\underline{R}_0| \qquad (3.2)$$

is the free-space Green's function; $\rho$ is the density of the exterior fluid whose sound velocity is c and whose acoustic wavenumber is $k = \omega/c$. The geometry is shown in Figure 1a.

Problems associated with a proper implementation, which is unique at all frequencies, have been analysed by Burton for the separate cases of general [4] and axisymmetric surfaces [5]. Computer implementation is not straightforward due to the presence of strongly singular integrals, which are difficult to evaluate numerically. It is the author's impression that implementations discussed in the literature either ignore or do not treat properly these singularities. Because the integrands are integrable the singularities may be ignored, but not safely because the resulting computer programs may be unreliable as well as inefficient. A recent publication by Reut [6] presents formulae which remove the problem of singular integrals for the case of flat rectangular surface elements over which the pressure and displacement can be regarded as constant.

(b) Axisymmetric Surface

For the specific case of the axisymmetric surface with the pressure $p$ and normal displacement $W$ represented by Fourier series expansions in the circumferential coordinate, viz.

$$p(r,z,\phi) = \Sigma_{n=0}^{\infty} p_n(r,z)\cos(n\phi)$$

$$W(r,z,\phi) = \Sigma_{n=0}^{\infty} W_n(r,z)\cos(n\phi) \qquad (3.3)$$

a procedure which explicitly takes into account the nature of the singularity in the integrands has been recommended by Miller [7].

The Green's function is expanded as

$$G(\underline{R},\underline{R}_0) = \Sigma_{n=0}^{\infty} G_n(r,r_0,z-z_0,)\cos n(\phi-\phi_0) \qquad (3.4)$$

in which

$$G_n(r,r_0,z-z_0) = (e_n/\pi)\int_0^{\pi} [\exp(ikD)/D]\cos(n\phi)d\phi \qquad (3.5)$$

with $e_n=1$ for $n=0$, $e_n=2$ for $n=1,2,3,..$; and

$$D \equiv D(r,r_0,z-z_0) = \{(z-z_0)^2+r^2+r_0^2-2rr_0\cos(\phi)\}^{1/2} \qquad (3.6)$$

The normal derivative of the Green's function, viz.

$$\partial G/\partial N_0 = \Sigma_{n=0}^{\infty} [\partial G_n/\partial N_0]\cos n(\phi-\phi_0) \qquad (3.7)$$

is obtained from the formula

$$\partial G_n/\partial N_0 = \cos(\beta)\partial G_n/\partial r_0 - \sin(\beta)\partial G_n/\partial z_0 \qquad (3.8)$$

in which the 'normal' angle $\beta$ is defined in Figure 1a. Thus,

$$\partial G_n/\partial N_0 = (e_n/\pi)\int_0^\pi (ik-1/D)\{\exp(ikD)/D^2\} \times$$
$$\{(r_0-r.\cos\phi)\cos\beta-(z_0-z)\sin\beta\}\cos(n\phi)d\phi \quad (3.9)$$

Noting that the area element on the surface, after first performing the $\phi_0$ integration, is

$$dS_0 = (2\pi/e_n)(r_0/\cos\beta)dz_0 \quad (3.10)$$

enables the Helmholtz integral equation to be written in terms of the harmonic amplitudes as

$$q(r,z)p_n(r,z) = (1/2e_n)\int \{p_n(r_0,z_0)\partial G_n(r,r_0,z-z_0)/\partial N_0$$
$$-\rho\omega^2 W(r_0,z_0)G_n(r,r_0,z-z_0)\}(r_0/\cos\beta)dz_0 \quad (3.11)$$

The integral runs over the axial length of the surface.

(c) Discretization

Let the field point $(r,z)$ be on the surface, which is divided into m-1 bands, as in Figure 1b, with ends at $z_i$, $i=1,m$. Thus $q(r,z)$ is 0.5 in equation (3.11), giving

$$-p_n(r,z) + (1/e_n)\sum_{i=1}^{m-1}\int \{p_n(r_0,z_0)\partial G_n(r,r_0,z-z_0)/\partial N_0\}(r_0/\cos\beta)dz_0$$
$$= (\rho\omega^2/e_n)\sum_{i=1}^{m-1}\int W(r_0,z_0)G_n(r,r_0,z-z_0)(r_0/\cos\beta)dz_0 \quad (3.12)$$

Along the generator of any element let the acoustic pressure and normal displacement vary linearly with the axial coordinate, $z_0$, viz.

$$p_n(r_0,z_0) = (z_{i+1}-z_i)^{-1}[z_{i+1}-z_0, -z_i+z_0]\begin{bmatrix}p_i\\p_{i+1}\end{bmatrix}$$
$$W_n(r_0,z_0) = (z_{i+1}-z_i)^{-1}[z_{i+1}-z_0, -z_i+z_0]\begin{bmatrix}W_i\\W_{i+1}\end{bmatrix} \quad (3.13)$$

where $p_i$ and $p_{i+1}$ are the values of the surface pressure harmonic, $p_n$, at the ends of the element; and $W_i$ and $W_{i+1}$ are the values of the normal displacement harmonic, $W_n$, at the ends of the element.

Substitute equation (3.13) into equation (3.12) to give the matrix equation

$$-p_n(r,z)+\sum_{i=1}^{m-1}\{[a(r,z),b(r,z)]\begin{bmatrix}p_i\\p_{i+1}\end{bmatrix}-[c(r,z),d(r,z)]\begin{bmatrix}W_i\\W_{i+1}\end{bmatrix}\} \tag{3.14}$$

in which

$$\begin{aligned}
a(r,z) &= h\int (z_{i+1}-z_0)\{\partial G_n(r,r_0,z-z_0)/\partial N_0\}(r_0/\cos\beta)dz_0\\
b(r,z) &= h\int (-z_i+z_0)\{\partial G_n(r,r_0,z-z_0)/\partial N_0\}(r_0/\cos\beta)dz_0\\
c(r,z) &= \rho\omega^2 h\int (z_{i+1}-z_0)G_n(r,r_0,z-z_0)(r_0/\cos\beta)dz_0\\
d(r,z) &= \rho\omega^2 h\int (-z_i+z_0)G_n(r,r_0,z-z_0)(r_0/\cos\beta)dz_0
\end{aligned} \tag{3.15}$$

with $h=(z_{i+1}-z_i)^{-1}/e_n$, the integration limits being $z_i$ and $z_{i+1}$.

If equation (3.14) is written down at the m values of (r,z) which correspond to the surface nodes, then a matrix equation results which relates the surface pressure and displacement at the m surface nodes, viz.

$$\underset{m*m}{[B(\omega)]}\ \underset{m*1}{[p]} = \underset{m*m}{[C(\omega)]}\ \underset{m*1}{[W]} \tag{3.16}$$

The inverse

$$\underset{m*1}{[p]} = \underset{m*m}{[B(\omega)]^{-1}}\underset{m*m}{[C(\omega)]}\ \underset{m*1}{[W]} = \underset{m*m}{[D(\omega)]}\ \underset{m*1}{[W]} \tag{3.17}$$

of this equation gives the surface pressure matrix in terms of the normal displacement matrix.

The integrals in equation (3.12) must be evaluated with some care as they are singular (but integrable). Details of their numerical evaluation, based on Miller's work [7], are to be given elsewhere.

## 4. COUPLED FE AND HIE

The matrix equation of motion is

$$\underset{m*m}{[S_e(\omega)]}\ \underset{m*1}{[W]} = \underset{m*1}{[F_E]} + \underset{m*1}{[F_p]} \tag{4.1}$$

where $[F_E]$ are the mechanical excitations, and $[F_p]$ are the forces due to fluid pressure which are obtained from the nodal point fluid pressures by the relation

$$\underset{m*1}{[F_p]} = -\underset{m*m}{[A]}\ \underset{m*1}{[p]} \tag{4.2}$$

where [A] is a frequency independent area matrix that converts nodal pressures to nodal forces.

The equivalent nodal point forces, due to fluid pressure, on the ith element are obtained by a standard finite element procedure. For linear variation of both displacement and pressure they are

$$\begin{bmatrix} F_i \\ F_{i+1} \end{bmatrix} = -(2\pi/e_n) \int \begin{bmatrix} c_1^2 & c_1c_2 \\ c_1c_2 & c_2^2 \end{bmatrix} \begin{bmatrix} p_i \\ p_{i+1} \end{bmatrix} (r_0/\cos\beta)dz_0 \tag{4.3}$$

where

$$\begin{aligned} c_1 &= (z_{i+1}-z_i)^{-1}(z_{i+1}-z_0) \\ c_2 &= (z_{i+1}-z_i)^{-1}(-z_i+z_0) \end{aligned} \tag{4.4}$$

and the range of integration is $z_i$ to $z_{i+1}$. Assembly of the element force matrix, equation (4.3), over all the elements gives the frequency independent triple-diagonal area matrix, [A].

Combining equations (4.1) and (4.2) gives the matrix equation of motion as

$$\underset{m*m}{[S_e(\omega)]}\ \underset{m*1}{[W]} = \underset{m*1}{[F_E]} - \underset{m*m}{[A]}\ \underset{m*1}{[p]} \tag{4.5}$$

which is now made specific to either mechanical excitation or acoustic excitation.

## 5. MECHANICAL EXCITATION

### (a) Response

Expand the mechanical excitation stress in the normal direction as a Fourier series, viz.

$$F(r_0,z_0,\phi_0) = \Sigma_{n=0}^{\infty} F_n(r_0,z_0)\cos(n\phi_0) \tag{5.1}$$

where

$$F_n(r_0,z_0) = (e_n/2\pi) \int_0^{2\pi} F(r_0,z_0,\phi_0)\cos(n\phi_0)d\phi_0 \tag{5.2}$$

For the specific case of a point force, $F_0$, located at one of the nodes, j say, at $\phi=0$

$$F(r_0,z_0,\phi_0) = F_0\delta(\phi)\delta(z_0-z_j)(\cos\beta/r_0) \tag{5.3}$$

the harmonic amplitudes are obtained from equation (5.2) as

$$F_n(r_0,z_0) = (e_n F_0 \cos\beta/2\pi r_0)\delta(z_0-z_j) \tag{5.4}$$

which can be shown to correspond, using equation (4.3) and the standard sign convention which requires positive values of stress and pressure to act in opposite directions at a surface, to a force vector, $[F_E]$, which has all zero elements except for the j'th which is simply $F_0$ for all harmonics.

The fluid pressure caused by the shell's vibrations must satisfy the the Helmholtz integral equation; and thus the matrix relation equation (3.17), which when substituted into equation (4.5) gives the coupled equations of motion as

$$\underset{m*m}{\Big[[S_e(\omega)]+[A][D(\omega)]\Big]}\underset{m*1}{[W]} = \underset{m*1}{[F_E]} \tag{5.5}$$

and it should be noted that the coefficients of the m*m matrix are neither symmetric nor banded, because the matrix $[D(\omega)]$ has been derived from an integral equation rather than an energy variational principle.

Inversion of the matrix equation (5.5) gives the 'normal' displacement response [W] in the n'th harmonic. The surface pressure [p] in the n'th harmonic is found from equation (3.17).

(b) Far-Field Sound Radiation

Approximating the Green's function and its derivative, in equations (3.5) and (3.9) by their values for a large 'D' gives the stationary phase approximation to the far-field pressure in the n'th harmonic (after much algebra) as

$$p_{nf}(R,\theta,\phi) = \overline{Y}_n(\alpha)(-i)^n \exp(ikR)/2R \tag{5.6}$$

where

$$\overline{Y}(\alpha) = \int_{z_1}^{z_m} Y(z_0)\exp(-i\alpha z_0)dz_0 \tag{5.7}$$

with

$$Y(z_0) = (r_0/\cos\beta) \quad X \tag{5.8}$$

$$\Big[p_n(r_0,z_0)\{\gamma.\cos\beta.J_n'(\gamma r_0)+i\alpha.\sin\beta J_n(\gamma r_0)\}-\rho\omega^2 W_n(r_0,z_0)J_n(\gamma r_0)\Big]$$

$\gamma=k.\sin\theta$ and $\alpha=k.\cos\theta$ being the stationary phase wavenumbers.

The integral in equation (5.7) is easily evaluated by, for example, Gaussian quadrature, the surface pressure $p_n$ and the surface normal displacement $W_n$ being found by interpolation in a table of [p] and [W] values which are found as described above.

## 6. ACOUSTIC EXCITATION

### (a) General Excitation

It is convenient to express the total fluid pressure in the n'th harmonic as

$$p_n(r,z) = p_{inc}(r,z)+p_r(r,z)+p_e(r,z) \tag{6.1}$$

where $p_{inc}$ is the incident wave, $p_r$ is the acoustic pressure scattered as though the shell were rigid (and immovable) and $p_e$ is the pressure scattered by the shell's elastic motion. The total acoustic particle displacement, $W_n(r,z)$, in a direction normal to the surface is found from the acoustic momentum relation

$$\partial p_n(r,z)/\partial N_0 = \cos\beta.\partial p_n(r,z)/\partial r-\sin\beta.\partial p_n(r,z)/\partial z = \rho\omega^2 W_n(r,z) \tag{6.2}$$

The nodal pressures and particle displacements are given by the matrix relations

$$\begin{aligned} \underset{m*1}{[p]} &= \underset{m*1}{[p_{inc}]}+\underset{m*1}{[p_r]}+\underset{m*1}{[p_e]} \\ \underset{m*1}{[W]} &= \underset{m*1}{[W_{inc}]}+\underset{m*1}{[W_r]}+\underset{m*1}{[W_e]} = \underset{m*1}{[W_e]} \end{aligned} \tag{6.3}$$

Note that the rigid body pressure is such that $[W_r] = -[W_{inc}]$, which means that it can be thought of as that pressure which arises from a virtual displacement $-[W_{inc}]$ normal to the surface. The particle displacement $[W_{inc}]$ is found from the discretized version of equation (6.2) in which $p_n(r,z)$ is set to $p_{inc}(r,z)$ and $W_n(r,z)$ to $W_{inc}(r,z)$. Thus $[p_{inc}]$, $[W_{inc}]$ and hence $[W_r]$ are all known.

The nodal surface pressure and displacement of the rigid body motion (suffix r) and the elastic motion (suffix e) must be solutions of the Helmholtz integral equation. Thus from equation (3.17)

$$\underset{m*1}{[p_r]} = \underset{m*m}{[D(\omega)]}\ \underset{m*1}{[W_r]} \tag{6.4}$$

is the (now) known matrix of of 'rigid' nodal pressures, and

$$\underset{m*1}{[p_e]} = \underset{m*m}{[D(\omega)]}\ \underset{m*1}{[W_e]} \tag{6.5}$$

is the matrix relation which connects the unknown 'elastic' nodal pressures and displacements.

From equation (4.5), setting $[F_E]=0$, together with the first of equations (6.3)

$$[S_e(\omega)]\,[W] = -[A]\,[p_{inc}+p_r+p_e] \tag{6.6}$$

Substitute equation (6.5) into this equation to give the fundamental fluid-structure matrix equation of motion for sound scattering as

$$\underset{m*m}{\Big[[S_e(\omega)]+[A][D(\omega)]\Big]}\;\underset{m*1}{[W]} = -\underset{m*m}{[A]}\;\underset{m*1}{[p_{inc}+p_r]} \tag{6.7}$$

and it is evident that for the case of acoustic excitation the driving force is the equivalent force due to the 'blocked' acoustic pressure.

Inversion of equation (6.7) gives the total nodal point displacement $[W] = [W_e]$, and hence the 'elastic' nodal pressure matrix, $[p_e]$, from equation (6.5). The scattered pressure and its normal displacement at the surface nodes are simply defined as

$$\begin{aligned}[p_s] &= [p_r]+[p_e]\\ [W_s] &= [W_r]+[W_e] = -[W_{inc}]+[W_e]\end{aligned} \tag{6.8}$$

The pressure scattered to the acoustic far-field is found from equations (5.6-5.8) in which $p_n(r_0,z_0)$ and $W_n(r_0,z_0)$ are found by interpolation in the table of nodal point values of equation (6.8). A frequently used reference is the pressure scattered to the far-field by the shell assumed to be rigid: this is obtained from equations (5.6-5.8), using $[p_r]$ and $[W_r]$.

(b) Plane Wave Excitation

Let the shell be insonified by the plane wave

$$p_{inc}(x,y,z) = P_i\exp\{ik(x.\sin\theta_i-z.\cos\theta_i)\} \tag{6.9}$$

which is incident at the angle $\phi_i=180°$, see Figure 1a. Its expansion in cylindrical coordinates is [8]

$$p_{inc}(r,z,\phi) = P_i\exp(-ikz.\cos\theta_i)\Sigma_{n=0}^{\infty}\, e_n i^n J_n(kr.\sin\theta_i)\cos(n\phi) \tag{6.10}$$

From now on the summation sign and the cos(n$\phi$) factor will be dropped because the analysis herein refers to the harmonic amplitudes only. Thus the incident pressure is

$$p_{inc}(r,z) = P_i \exp(-ikz.\cos\theta_i) e_n i^n J_n(kr.\sin\theta_i) \qquad (6.11)$$

whose particle displacement is obtained from equation (6.2), with $p_{inc}$ substituted for $p_n$, as

$$W_{inc}(r,z) = (1/\rho\omega^2)\exp(-ikz.\cos\theta_i) e_n i^n \times \qquad (6.12)$$
$$\{k.\sin\theta_i J_n'(kr.\sin\theta_i)\cos\beta + ik.\cos\theta_i J_n(kr.\sin\theta_i)\sin\beta\}$$

All the ingredients are now present to enable computation of the scattered pressure field. The procedure to be followed is the same as for the general excitation case, which is described above.

## 7. NUMERICAL TESTS

### (a) General

Fortran programs have been written for calculating the far-field pressure from an axisymmetric shell structure (with or without branches and ribs) which is excited by either a time-harmonic mechanical point force, or by a time-harmonic plane wave which is incident at an arbitrary elevation angle. The field quantities, of course, are represented by Fourier series expansions in the circumferential coordinate.

Miller [7] has shown that that the integral representations of the Green's function and its derivative, equations (3.5) and (3.9) introduce logarithmic singularities in the kernel of the integral equation (3.11), at the point $(r_0,z_0)=(r,z)$, and goes on to develop quadrature formulae which explicitly treat these singularities. However, because the singularities are logarithmic, they may be integrated, although inefficiently, by Gaussian quadrature. The penalty of course is that the computation time needed to achieve a given accuracy increases several times. The current versions of the programs use Gaussian quadrature, thus effectively ignoring the singularity except for vastly increasing the quadrature points on singular elements. A future publication will show the value of treating these singularities properly and it will also describe an attempt to improve the integration over end elements, which turned out to be troublesome.

### (b) Spherical Shell Constants

As a first test of the correctness of the Fortran programs numerical results of sound radiation from and sound scattering by a thin empty spherical steel shell, submerged in water, are compared with those obtained from closed-form expressions derived from a shell theory [9,10]. The material and geometric constants in SI units are as follows:

Shell: Young's modulus $19.5\text{x}10^{10}$
Poisson's ratio 0.29

Density 7700.0
Thickness 0.01
Radius 1.0
Hysteretic loss-factor 0.01

Water: Density 1000.0
Sound velocity 1500.0

(c) Spherical Shell Test of n=0

Figure 2 shows radiated sound levels when the shell is excitated by a 'normal' point force located on the z-axis. Thus both the geometry and the excitation are axisymmetric, which means that only the n=0 harmonic contributes to the far-field radiation, calculated at $\theta=0$. In Figure 2a the shell was divided into 20 conical shell elements, with a constant angular spacing of 9°. Agreement with the 'exact' solution is good up to the frequency of the first resonance; thereafter the finite element levels are seriously in error, although the frequencies at which resonances occur are reasonably accurate. In Figure 2b the shell was divided into 40 conical shell elements with an angular spacing of 4.5°. Agreement with the exact solution has improved dramatically.

Figure 3 shows plots of monostatic target strength, the excitation being an axial plane wave. Again both the geometry and the excitation are axisymmetric, which means that only the n=0 harmonic contributes to the target strength. In Figure 3a the shell was divided into 20 conical shell elements, with a constant angular spacing of 9°. Agreement with the 'exact' solution is very good up to the frequency of the second resonance; thereafter the finite element levels are in error, but not as seriously as those in Figure 2a. The shell was divided into 40 conical shell elements with an angular spacing of 4.5° in Figure 3b. Agreement with the exact solution has improved, as expected, and is satisfactory over all the frequency range.

Also shown in Figure 3 is the sound scattered by a rigid sphere. There is no distinguishable difference between the 'exact' curve and the levels derived (in this case) from the Helmholtz integral equation alone.

The numerical results discussed have demonstrated that the problem formulation and computer programs must be substantially correct, at least for the n=0 harmonic. They also suggest that the weak link in the numerical formulation is more likely to be in the finite element part rather than in the Helmholtz integral equation implementation. No substantiated explanation is offered as to why the numerical results of sound scattering are more accurate than those of acoustic radiation, for a given idealisation. Perhaps it is related to the accuracy of the off-diagonal elements of the shell's receptance matrix being more accurate than the diagonal elements.

(d) Spherical Shell Test of n=0-3

The implementation of the Helmholtz integral equation should fail at the forbidden frequencies, which are the eigenvalues of the associated interior problem with Dirichlet boundary condition

on the surface. Practically, this means that the numerical inversion of the matrix [B] defined by equation (3.16) will become more and more ill-conditioned as a forbidden frequency is approached. For the sphere the forbidden frequencies are simply the roots of the equation, $j_n(ka)=0$, which are f=750 for n=0, f=1072 for n=1, f=1376 for n=2 ... Numerical tests did indeed show severe ill-conditioning as these critical frequencies were approached.

As a test of the full formulation for general 'n' it is useful to consider the sound scattered by the spherical shell when it is excited by a plane wave incident at $\theta_i=90°$. In this case the monostatic target strength is a combination of all harmonics. Because of symmetry, it must be the same (at least theoretically) as the monostatic target strength of the shell when it is excited at $\theta=0°$, which involves the n=0 harmonic alone. The following table, in which R denotes scattering from a rigid body and E denotes scattering from the spherical elastic shell, is a comparison of monostatic target strength levels in decibels at selected frequencies:

| Frequency Hz | Exact | | θ=0° (n=0) | | θ=90° (n=0-3) | |
|---|---|---|---|---|---|---|
| | R | E | R | E | R | E |
| 100 | -17.5 | -19.9 | -17.5 | -19.9 | -17.5 | -19.9 |
| 150 | -11.5 | -13.0 | -11.5 | -13.0 | -11.5 | -13.0 |
| 200 | -8.0 | -7.6 | -8.0 | -7.7 | -8.0 | -7.6 |
| 250 | -6.3 | 1.0 | -6.4 | 0.4 | -6.3 | 0.9 |
| 300 | -6.2 | -4.8 | -6.3 | -3.8 | -6.2 | -4.2 |

For $\theta=90°$ numerical tests showed that it was sufficient to sum from n=0 to 3 only. The main contribution comes from the n=1 harmonic and the n=0 harmonic is significant also; the n=2 harmonic contributes significantly at 200, 250 and 300Hz, and the n=3 harmonic is significant only at 300Hz. The 'rigid' body levels (R) agree to within 0.1dB at all frequencies, which demonstrates that the solution of the Helmholtz integral equation is also credible at values of 'n' other than n=0. The spherical shell levels (E) agree to within 0.1dB at 100, 150 and 200Hz, and to within 1dB at frequencies 250 and 300Hz which are either side of a resonance. Overall these results help considerably to reinforce the opinion that the programs could be a useful tool for solving certain low frequency radiation and scattering problems.

## 8. CONCLUDING REMARKS

A receptance method for calculating the exterior acoustics of axisymmetric shell structures has been presented. The method is relatively economical in computer time because 'normal' coordinates alone are used for the fluid-structure coupling. The method has been validated by comparing numerical results obtained from the formulation with 'exact' results obtained from a closed-form expression.

Much theoretical work remains to be done before a practical and robust suite of programs is available, but it is thought that

the programs developed so far are a useful tool for obtaining numerical results of sound radiation and scattering for research purposes. Future work in this area should include (a) a proper treatment of the singular integrals in the Helmholtz integral equation, according to Miller's analysis [7]; and an implementation of a quadratic isoparametric element to replace the linear element used herein; (b) a theoretical analysis of the additional singular integral which would occur if it were thought desirable to implement the full Burton and Miller method, described in Burton [4,5]; and (c) the use of a quadratic isoparametric conical shell element, as the numerical results have suggested that the finite element part is the weakest link in the formulation.

## 9. ACKNOWLEDGEMENT

Thanks are due to G.F. Miller of the National Physical Laboratory, Teddington, for valuable advice on the numerical implementation of the Helmholtz integral equation.

J.H. James (PSO)
July 1987.

# REFERENCES

1. James J.H., Coupled FE and HIE method for exterior acoustics of slender axisymmetric shells (I) Preliminary study axisymmetric excitation, Admiralty Research Establisment, Teddington, ARE TM(UHA)86517, Unpublished MoD(PE) Report, October 1986.

2. James J.H., Vibration analysis of axisymmetric structures: Fortran computer program specifications, Admiralty Research Laboratory, Teddington, ARL/R/P1, November 1972. (An updated specification is available).

3. Percy J.H., et al, Application of matrix displacement method to linear elastic analysis of shells of revolution, AIAA Journal, 3(11), 1965, pages 2138-2145.

4. Burton A.J., Numerical solution of acoustic radiation problems, National Physical Laboratory, Teddington, Contract Report NAC 0C5/535, February 1976.

5. Burton A.J., Acoustic radiation by axisymmetric surfaces with arbitrary data, National Physical Laboratory, Teddington, Contract Report NAC 92/615/0C, March 1978.

6. Reut Z., On the boundary integral methods for the exterior acoustic problem, J.Sound.Vib., 103(2), 1985, pages 297-298.

7. Miller G.F., A note on the solution of certain integral equations, National Physical Laboratory, Teddington, Unpublished work for ARE Teddington, February 1987.

8. James J.H., Sound scattering from infinite fluid-filled cylindrical shell, Admiralty Marine Technology Establishment, Teddington, AMTE(N)TM83107, October 1983.

9. James J.H., Intensity vectors of sound scattering by a spherical shell, Admiralty Marine Technology Establishment, Teddington, AMTE(N)TM84080, July 1984.

10. James J.H., Fortran program for vibration and sound radiation of spherical shell, Admiralty Research Establishment, Teddington, ARE TM(N1)86501, January 1986.

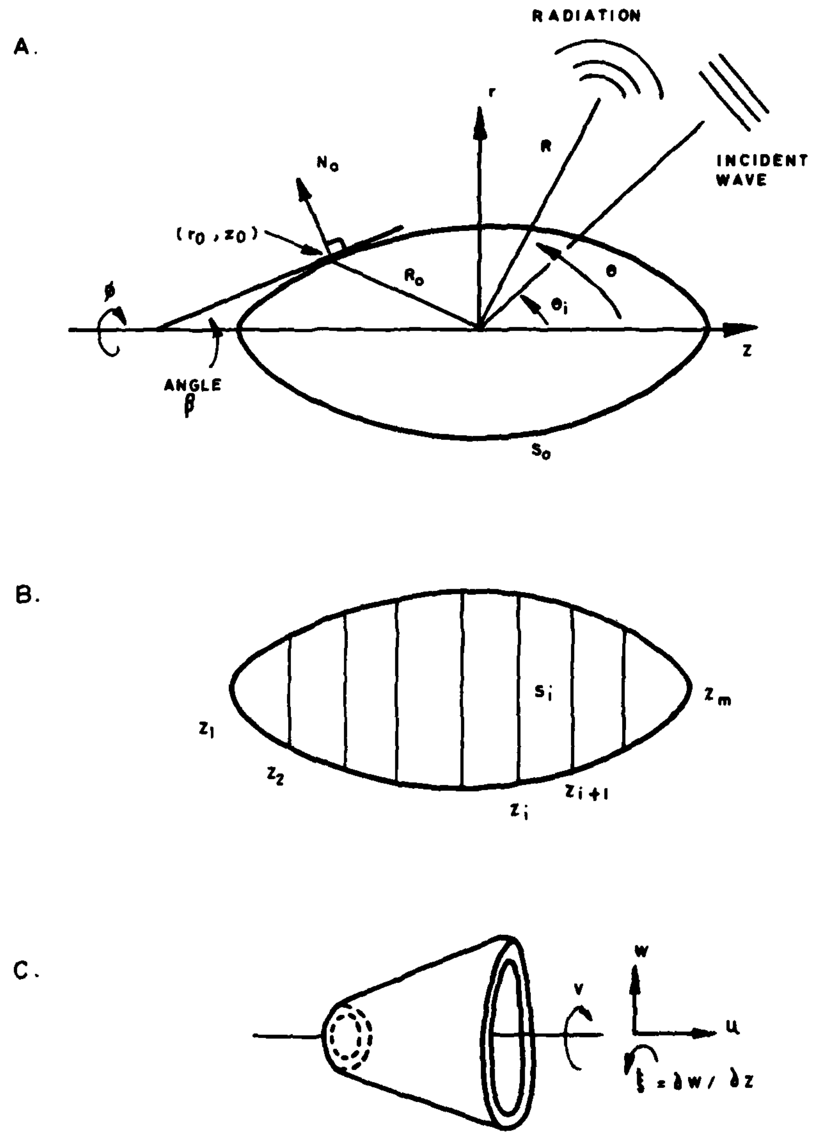


FIG. 1 (A) GEOMETRY (B) SUBDIVISION (C) SHELL ELEMENT

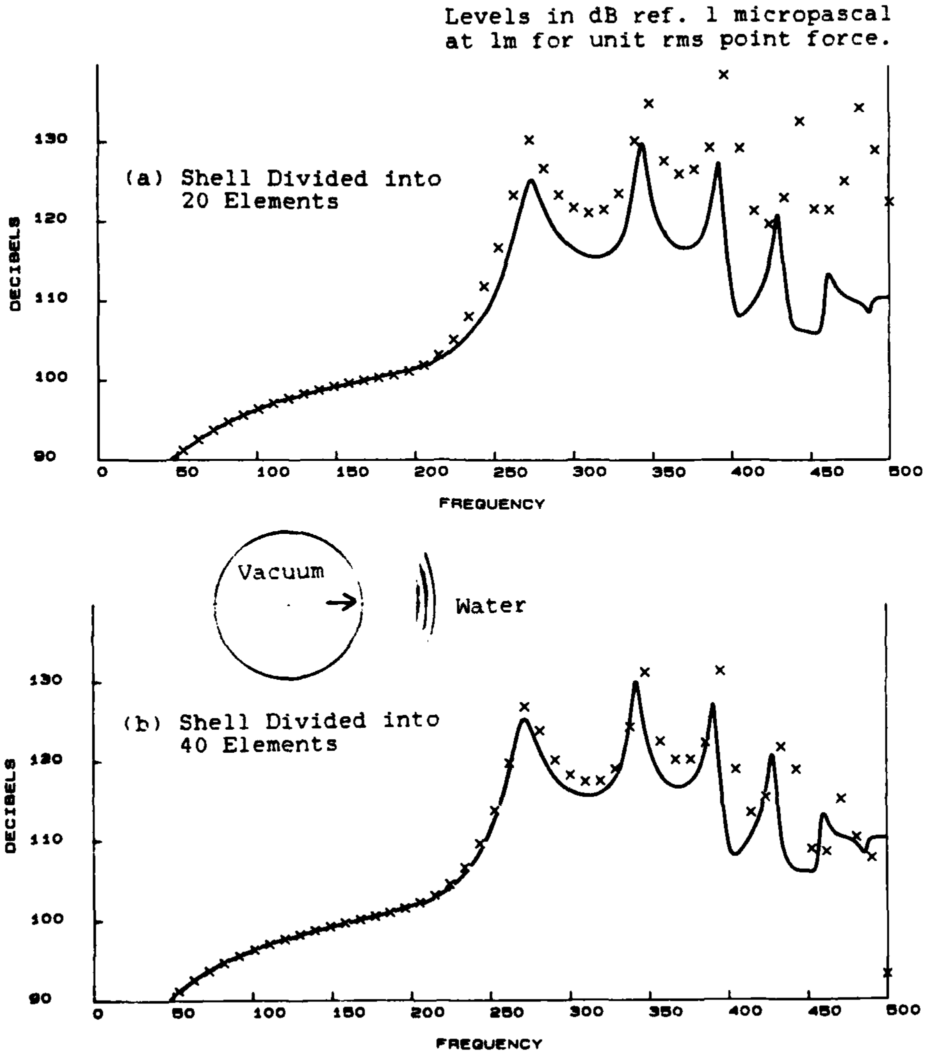


FIG. 2 FAR-FIELD SOUND RADIATION FROM SPHERICAL SHELL
—— exact; x finite element

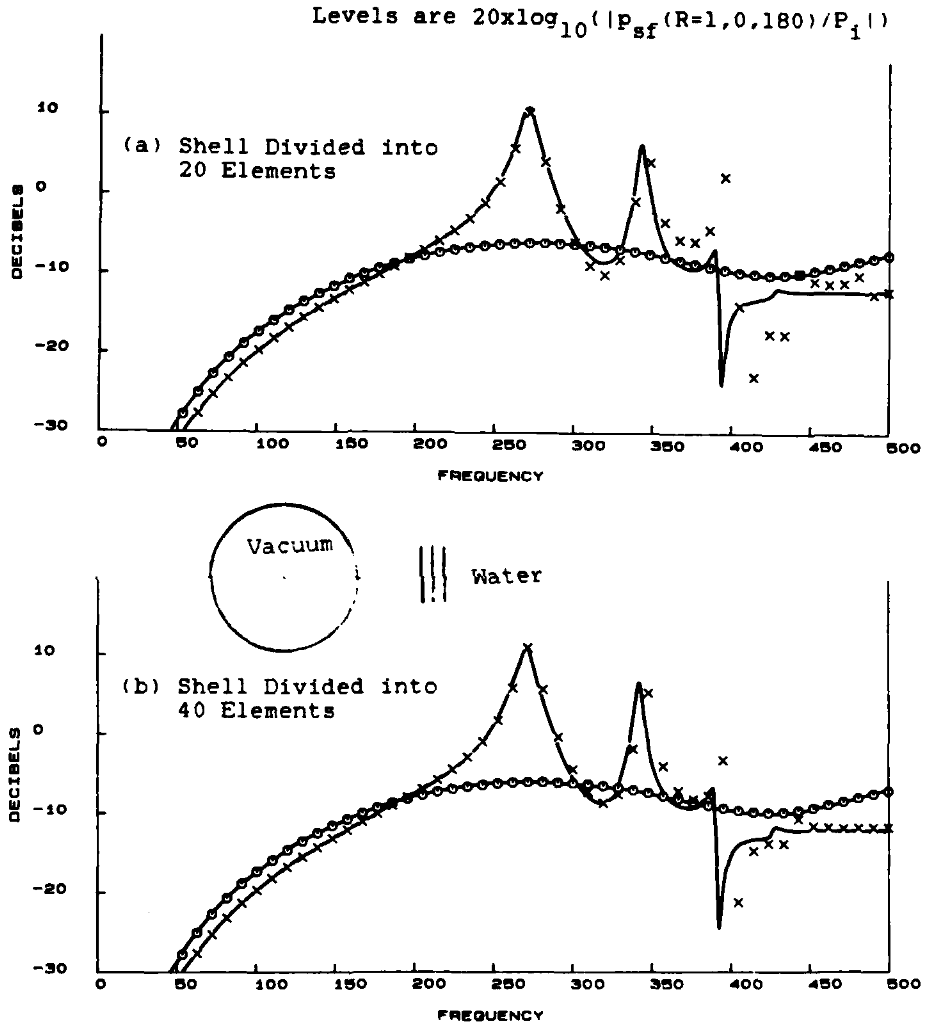


FIG. 3 MONOSTATIC TARGET STRENGTH OF SPHERICAL SHELL
— exact; x finite element; ⊙ rigid body

# END

## DATE FILMED

2 88